

MODULE 4: MODULE – 4: Biological, Chemical, and “Lab on a Chip” Sensors Electric, Magnetic, and RF/Microwave Sensors

Structure

4.1 Biological, Chemical, and “Lab on a Chip” Sensors: Lab on a Chip Sensors,

4.2 Other Biochemical Micro- and Nano-Sensors.

4.3 Electric, Magnetic, and RF/Microwave Sensors: Magnetic Field Sensors,

4.4 Other Important Electromagnetic/RF Micro- and Nano-Sensors..

Objectives

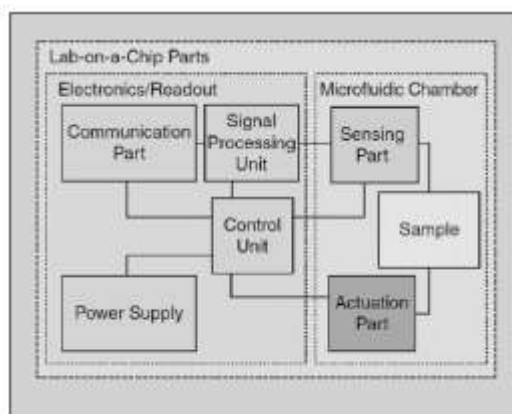
To explain the structure, operation of Biological Sensors, Chemical Sensors, and the so called “Lab-on-a-Chip” sensors used in multipurpose biological and chemical analysis devices and Electric, Magnetic, and Integrated Sensor/Actuator Units and Special Purpose Sensors driven by nanotechnology.

4.1 Biological, Chemical, and “Lab on a Chip” Sensors: Lab on a Chip Sensors

“Lab on a Chip” Sensors

Chemical and biological sensors have advanced tremendously during the past two decades thanks to the advances in nanotechnology and nanofabrication.

A lab-on-a-chip (LOC) is a device that integrates one or several laboratory functions on a single integrated circuit (commonly called a "chip") of only millimeters to a few square centimeters to achieve automation and high-throughput screening.

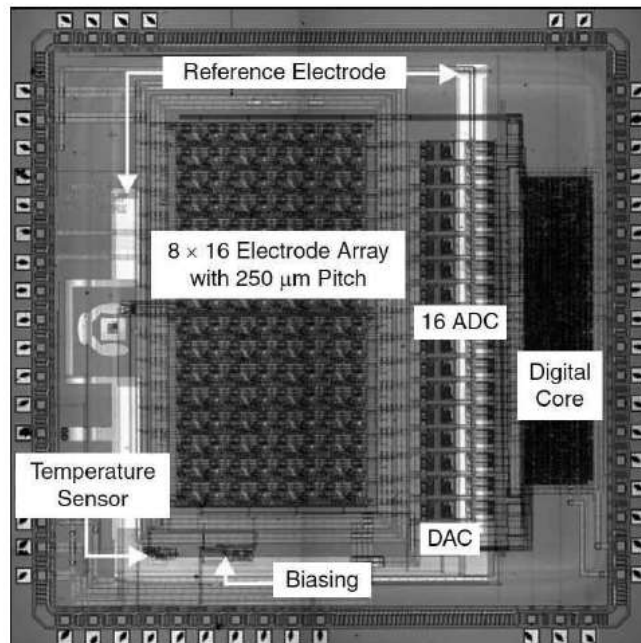


A Lab on a Chip is essentially composed of three sections:

- Actuation,
- Sensing and
- Electronic interface circuitry.

A scanning electron microscope (SEM) micrograph of an actual Lab on a Chip

- is shown in Figure

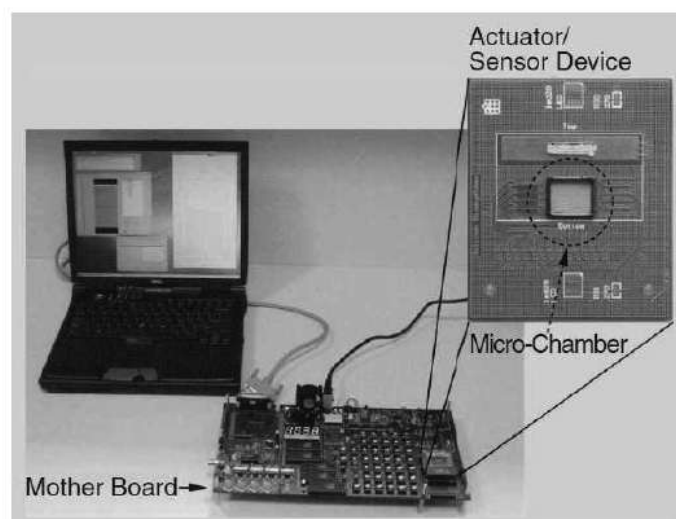


Step-1: In the actuation section, the chip generates electrical or mechanical forces that act on the biological sample (cells/fluid).

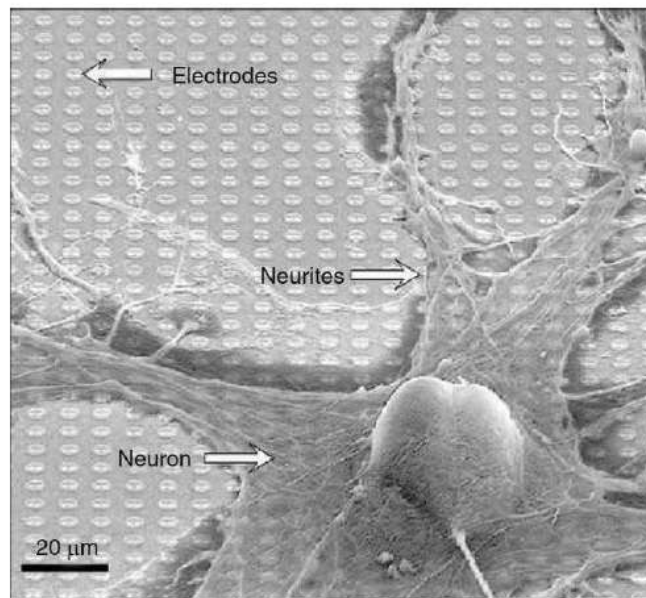
Step-2: In the sensing section, sensors that are embedded in the chip measure responses that may be electrical, optical, thermal, or magnetic, and route the detected signals to the electronic section for final processing.

Step-3: The electronic interface circuitry finally performs traditional signal processing functions such as amplification and noise reduction.

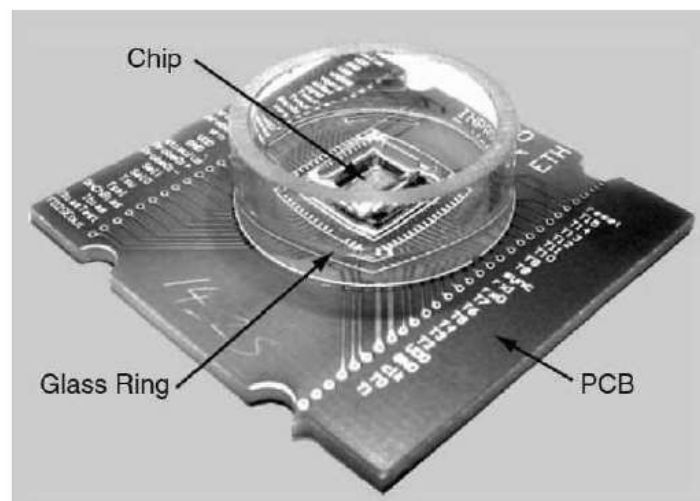
Lab on a Chip to a computer's data acquisition system.



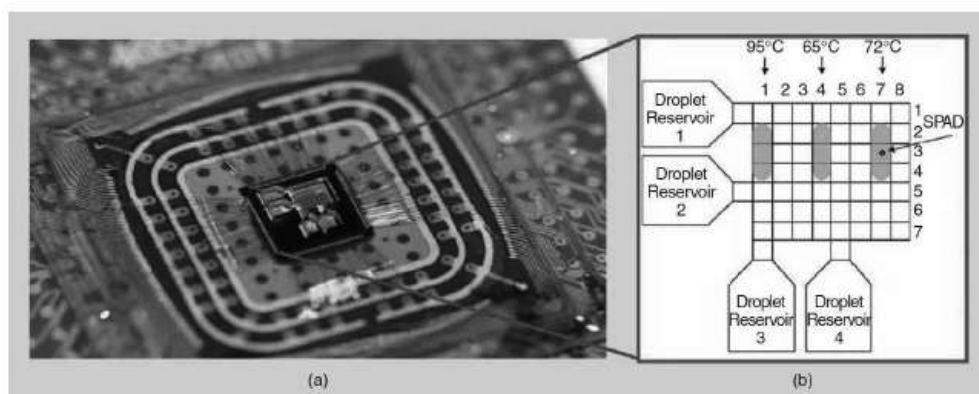
Neuron of a snail analyzed by a “Lab on a Chip”



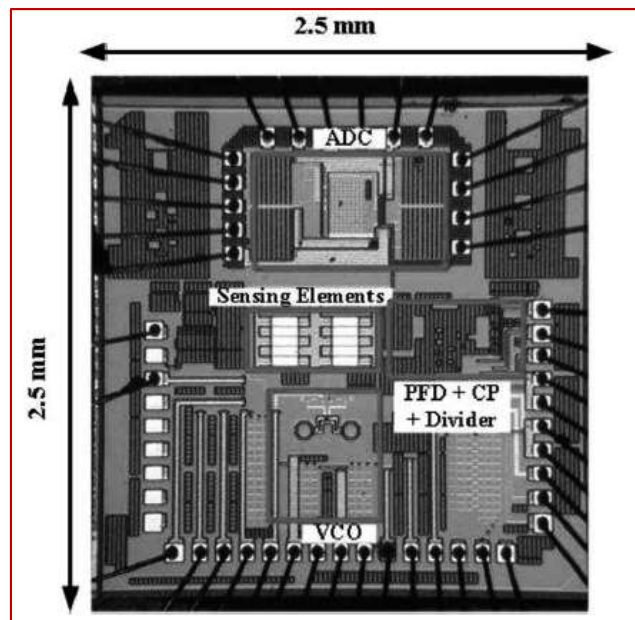
Typical packaging of a “Lab on a Chip”



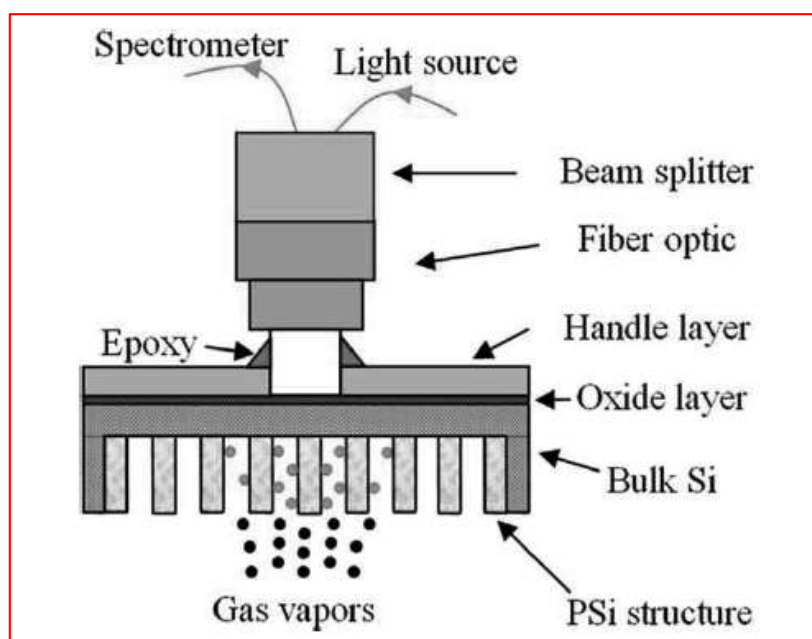
“Lab on a Chip” implemented directly on a printed circuit board



4. 2 Other Biochemical Micro- and Nano-Sensors



CMOS on-chip sensor for measuring the dielectric constant of organic chemicals



Porous silicon based sensor for chemical gas vapor detection,

4. 3 Magnetic Field Sensors

A new type of solid-state magnetic field sensor that is similar in size to a Hall effect sensor and that offers a sensitivity that is approximately an order of magnitude better than a Hall effect sensor was recently introduced

The significant advantage of the new sensor, however, is that it consumes no power

The sensor consists of a radioactive β -particle source and a silicon p-n junction.

If no magnetic field is applied, the β particles enter the p-n junction and generate a steady DC voltage

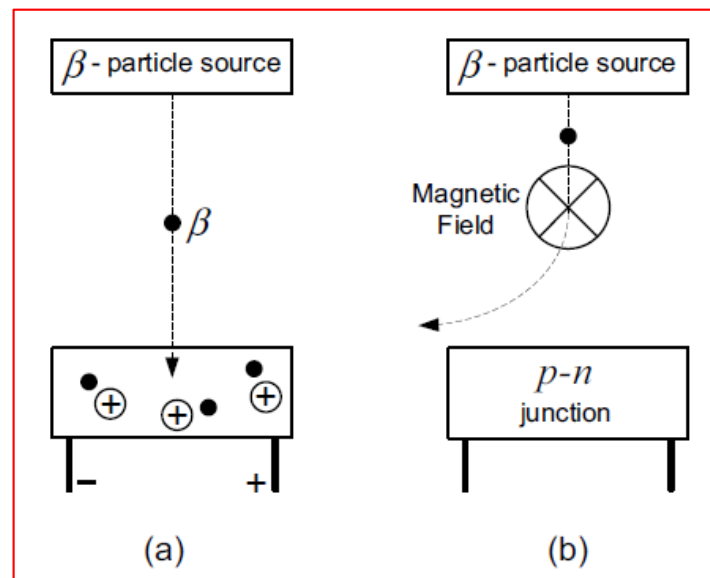
Under the influence of a magnetic field, however, the β particles (or secondary electrons generated therefrom) follow a curved path and miss the p-n junction, and the magnitude of the output voltage drops.

At the present time, however, the magnetic field sensor of choice in most industrial applications is still the traditional Hall effect sensor , due to its high sensitivity, small size, and low cost.

The Hall effect sensor is also increasingly being used in portable electronic devices, such as digital cameras and smart tablets.

Unfortunately, the traditional Hall effect sensor requires a current on the order of a few tens of mA to achieve its typical sensitivity, or about 10^{-4} T.

Principle of Operation



The new sensor depends on the beta-voltaic principle

Step-1: In Figure (a), a source of low energy β particles is positioned above a p-n junction.

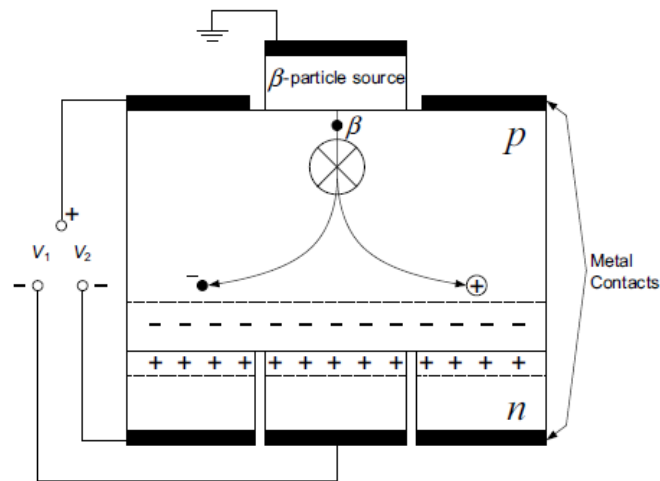
Step-2: As the β particles enter the p-n junction, electron-hole pairs are produced inside the junction, and a voltage appears across the terminals of the junction (the beta-voltaic principle is a well-known principle of physics)

Step-3: In Figure (b), a magnetic field is applied in a direction that is perpendicular to the direction of motion of the β particles (or high-speed electrons).

Step-4: As a result, the β particles follow a curved path and miss the p-n junction, and the voltage across the terminals of the junction therefore drops in magnitude.

Step-5: The β -particle source used in the new sensor is tritium, with a half-life of 12.3 years. Such a half-life will be acceptable for portable consumer products, which typically have comparable lifetimes

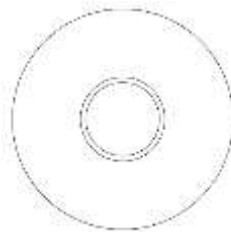
Step-6: β particles are high-speed electrons. Even if the source is a low-energy source such as tritium, the velocity of the β particles is substantially high (exceeds 10^7 m/s).



Cross-sectional view of the actual sensor (upper) and a projection view of the two n-doped regions (lower)

Step-1: As shown in Figure, the β -particle source is mounted immediately above a semiconductor body consisting of a p-type substrate and two n-doped regions.

Step-2: The two n-doped regions have the shape of concentric circles



Cross-sectional view of the actual sensor (upper) and a projection view of the two n-doped regions (lower)

Step-3: Two separate p-n junctions therefore exist in the device. The p-region has one metal contact, as shown in the figure, while the two n-regions have separate metal contacts.

Step-4: β particles emitted from the decay of tritium have a maximum energy of 18.6 keV and an average energy of 5.7 keV. These energetic β particles enter the p-type region, where they lose their kinetic energy within a distance of less than 1 μm

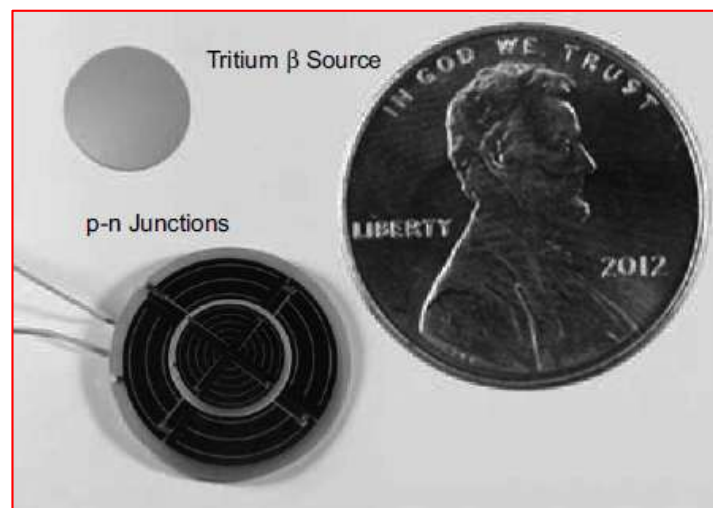
Step-5: If no magnetic field is applied, the newly created EHPs drift toward the depletion region in the center, where the internal electric field in the depletion region forces the electron toward the n-type material and forces the hole back into the p-type material.

Step-6: As a result, a voltage V_1 appears across the terminals of the inner p-n junction, while the voltage V_2 across the outer p-n junction will be

equal to 0.

Step-7: If, however, a magnetic field is applied in a direction that is perpendicular to the direction of motion of the β particles, the newly created EHPs (which have slow, nonrelativistic velocities) follow curved paths and accumulate on the sides of the p-substrate, as shown in the figure. Accordingly, the outer p-n junction receives a larger portion of the EHPs and the voltage V_2 increases, while V_1 falls. The interface circuit of the sensor is designed to detect the voltage differential $V_2 - V_1$

Figure shows a photograph of the two main components of the sensor:



The two components of the sensor: the tritium β source and the two concentric silicon p-n junctions.

The diameter of the larger component is 12 mm. One US penny is shown in the photograph for size comparison.

Theory

Range of the β particles in silicon:

The maximum range of penetration of a β particle into any material can be found from the Katz–Penfold formula

$$R_{max} = 0.412 E_{\beta}^{1.265 - 0.0954 \ln(E_{\beta})},$$

where R_{max} is the material-independent maximum range (in g/cm²)

E_{β} is the initial energy of the β particle in MeV

The maximum penetration distance in silicon will therefore be given by

$$R(\text{silicon}) = \frac{R_{max}}{\rho},$$

where $\rho = 2.33 \text{ g/cm}^3$ is the density of silicon

For an average kinetic energy $E_{\beta} = 5.7 \text{ keV}$, the formula predicts a penetration depth in silicon of $0.2 \text{ }\mu\text{m}$.

The penetration depth is therefore very small.

Bending radius of the generated free electrons:

Expressions for the

1. minimum initial kinetic energy of the electron,
2. its final kinetic energy, and the
3. radius of the arc along its trajectory.

minimum kinetic initial energy will be given by

$$\frac{1}{2}mv_0^2 = \int F dl$$

where F is the Lorentz force,

$$F = q(\vec{E} + \vec{v} \times \vec{B})$$

where F is the Lorentz force, given by $F = q(\vec{E} + \vec{v} \times \vec{B})$. Here, as usual, m is the electron's mass, \vec{v} is the electron's initial velocity, q is the electron's charge, \vec{E} is the steady-state electric field that will be present between the terminals of the device

$$\frac{1}{2}mv_0^2 = q \int \vec{E} \cdot d\vec{l} + q \int (\vec{v} \times \vec{B}) \cdot d\vec{l}$$

Since the magnetic force is always perpendicular to the path, it can be immediately seen that the second integral vanishes, and the above equation reduces to

$$\frac{1}{2}mv_0^2 = qV,$$

where V is the steady-state electrostatic potential, or voltage, between the terminals of the device

$$v_0 = \sqrt{\frac{2qV}{m}}$$

The terminal (or final) kinetic energy of the electron as it approaches the depletion region can be found as follows:

At steady-state (where electrons finally stop crossing the depletion region due to saturation of the p-n junction), the sum of the electron and hole currents must be equal to zero

$$J = nqv_e$$

where J is the current density, n is the free-electron density in the p-region, and v_e is the terminal velocity of the electron, we must therefore conclude that

$$nqv_e + pqv_h = 0$$

where p is the hole density and v_h is the hole's terminal velocity

$$v_e = -\frac{p}{n}v_h$$

Holes will be directly driven by the steady-state electric field present between the terminals of the device, and v_h will be therefore given by

$$v_h = \mu_h E$$

where μ_h is the hole's mobility

$$\begin{aligned} v_e &= -\frac{p}{n} \mu_h E \\ &= -\frac{p}{n} \mu_h \left(\frac{V}{L} \right) \end{aligned}$$

where L is the thickness of the device

In this application, electrons and holes are created in pairs. Since only these mobile carriers contribute to the current in the device, $n = p$

$$v_e = -\mu_h \left(\frac{V}{L} \right)$$

The negative sign merely indicates that the direction of motion of the electrons will be opposite to that of holes

the kinetic energy of the electron takes the form

$$\frac{1}{2}mv^2 = \frac{1}{2}mv_0^2 e^{-\alpha l}$$

where α is an attenuation constant.

total length l of the electron's path (before reaching the depletion region) is only slightly different from the overall thickness L of the device

Along its path, the electron is in equilibrium due to the equality of the magnetic and the centrifugal forces, that is,

$$qvB = \frac{mv^2}{R}$$

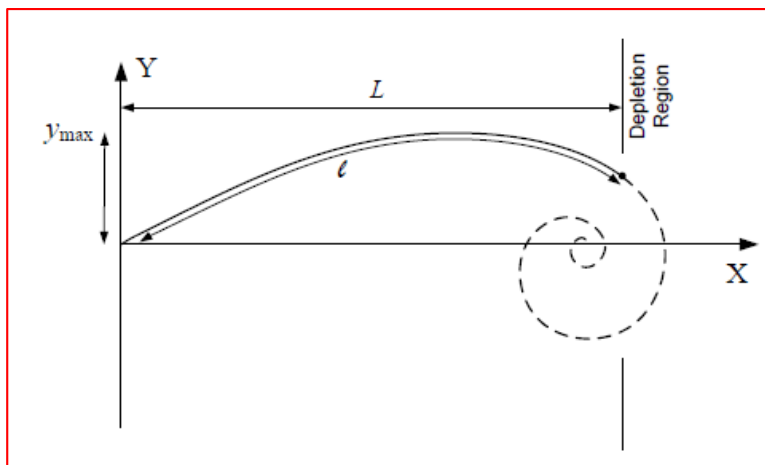
R will be given by

$$R = \frac{mv}{qB}$$

The final value of that radius can actually be determined with good accuracy: it can be immediately seen from the above equation that when $l = L$, the final radius of curvature will be given by

$$R = \frac{mv_e}{qB}$$

Simplified geometry of the logarithmic spiral curve in the present problem
(the curve is rotated 90° for clarity).



Manufacturing and Assembly of the Prototype Sensor

The tritium beta source was manufactured with relatively simple laboratory equipment.

Tritium is the only β -particle source that is suitable for this application because the maximum energy of the emitted β -particles is 18.6 keV, which is just below the threshold of energy at which damage to the atomic lattice in silicon would occur

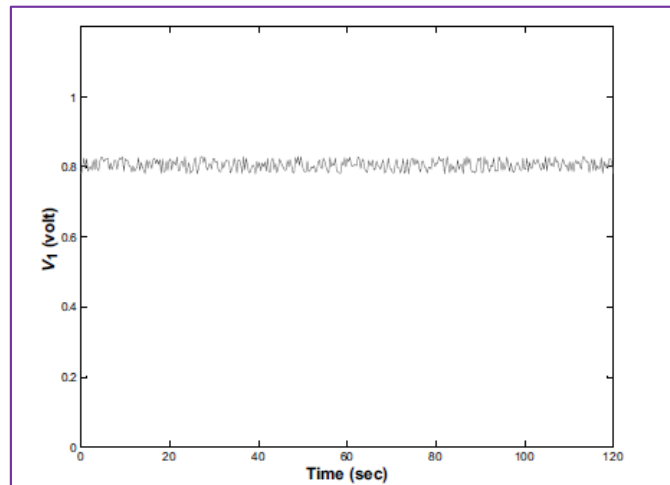
The process of embedding of tritium

Crystalline silicon disk is exposed to tritium gas at a pressure of about 120 atm and a temperature in the range of 250–300°C

The sample is typically exposed to 300°C for several days.

The tritium (in atomic form) diffuses inside the atomic silicon lattice up to a depth of approximately 10 nm

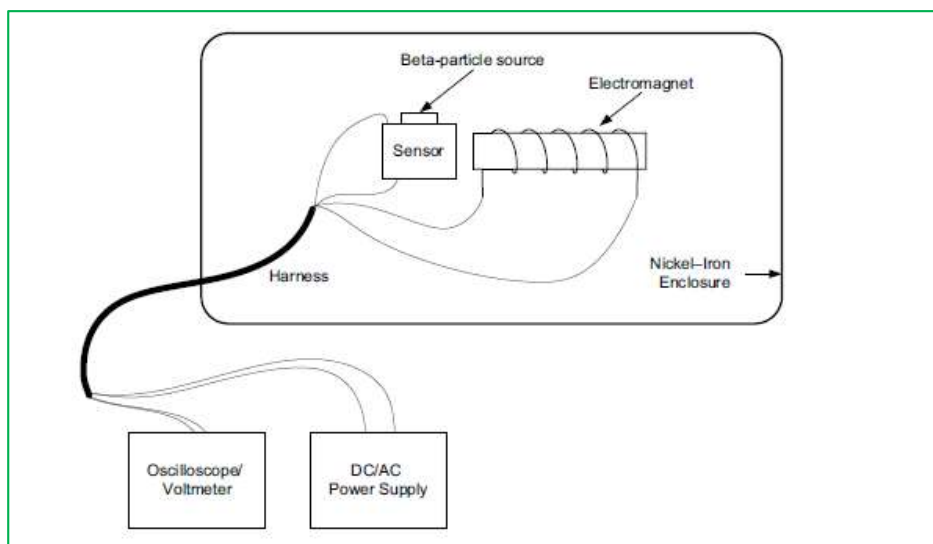
The tritium thus embedded in the silicon sample is usually found to be very stable at all temperatures below



The voltage V_1 produced by the inner p-n junction as a function of time

(with no applied magnetic field). The magnetic field of the earth was shielded by placing the experimental setup inside a nickel-iron enclosure

Diagram of the experimental setup for testing the sensor

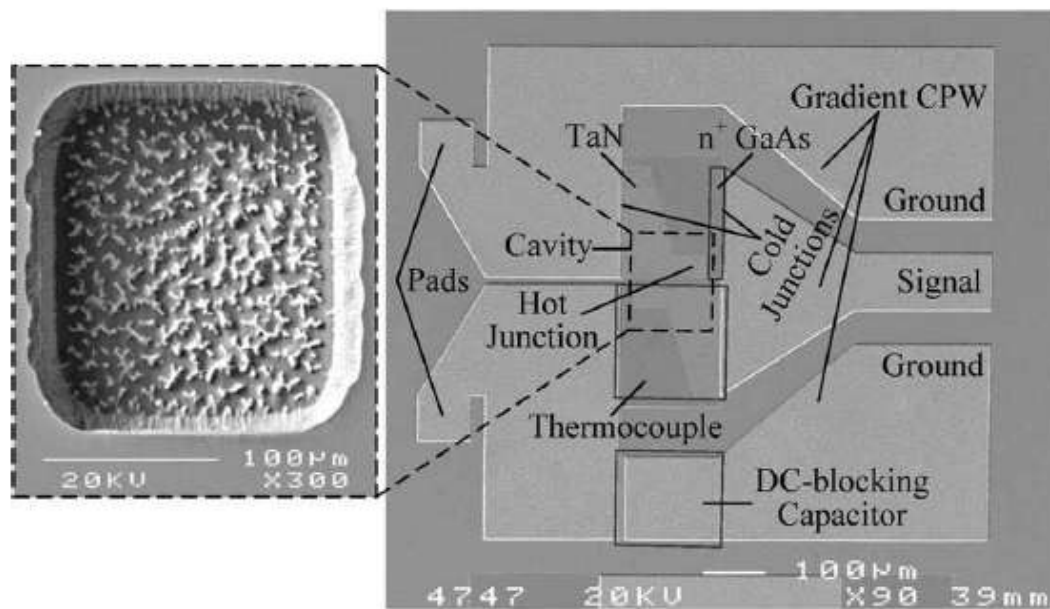


Temperature effect on the response of the sensor

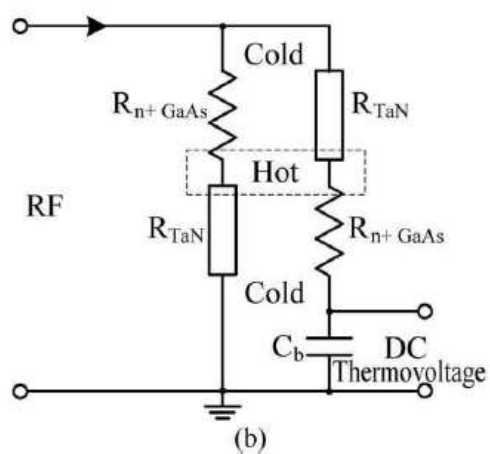
two tests that were conducted with a DC field at temperatures of -40°C and $+120^{\circ}\text{C}$.

Clearly, lower temperatures have only a minimal effect on the sensitivity of the sensor, while a significant deviation in the output voltage occurs at high

A thermocouple-based self-heating RF power sensor with GaAs MMIC-compatible micromachining technology



(a)



(b)

Outcomes

At the end of the module, students will be able to:

CO-4: Illustrate the working of biological, chemical & different electromagnetic sensors and construct its fabrication based on nanotechnology.

TEXT BOOKS:

1. Micro- and Nano-Scale Sensors and Transducers, By Ezzat G. Bakhoum, CRC Press, 1st Edition, 2015.

Reference Books

1. Electrical and Electronic Measurements, R.K Rajput, S. Chand, 3rd Edition, 2013
2. A Course in Electronics and Electrical, J.B. Gupta, Katson Books, 13th Edition, 2008
3. A Course in Electrical and Electronic Measurements and Instrumentation, A. K. Sawheny, Dhanpat Rai,
4. https://onlinecourses.nptel.ac.in/noc21_ee26/preview
5. <https://nptel.ac.in/courses/108108147>